Indian Journal of Chemistry
Vol. 61, September 2022, pp. 976-988
DOI: 10.56042/ijc.v61i9.60668

Structure-based drug designing of histone deacetylase-2 inhibitors as anticancer agents

Somya Bisht*[a], Anita Singh[a] & Naidu Subbarao[b]

[a] Department of Pharmaceutical Sciences, Bhimtal Campus, Kumaun University, Nainital 263 136, Uttarakhand, India

[b] School of Computational and Integrative Sciences, JNU, New Delhi 110 067, India

E-mail: bishtsumi30@gmail.com

Received 19 February 2022; revised (accepted) 18 July 2022

Histone deacetylase 2 (HDAC-2) in tumor development and carcinogenesis is a promising therapeutic target for cancer treatment. HDAC-2 belongs to class I histone deacetylase and acts as a transcriptional repressor through the deacetylation of lysine residues present at the N-terminal tail of histone proteins (H2A, H2B, H3, and H4). They are overexpressed in various solid tumors like cutaneous T cell lymphoma, colorectal cancer, prostate cancer, lung cancer, breast cancer, gastric cancer, liver cancer, and medulloblastoma. Hence, targeting HDAC-2 could be a rewarding strategy to combat cancer. The goal of the research is to design, develop, and identify molecules through docking, Ligplot, ADMET properties, and molecular dynamic studies. The compound CHEMBL4087539 has been observed to be a top scoring inhibitor against HDAC-2. The molecular dynamics simulation shows the convergence of ligand protein interaction. In the 100 ns, the ligand strongly interacts with HDAC-2. Furthermore, the ADME studies show the suitability of predicted inhibitor as a drug like molecule.

Keywords: Histone deacetylase, molecular dynamics, 4LY1, ADME property

Cancer is a disease in which abnormal growth of cancer cells divides uncontrollably, destroying body tissue. It goes beyond its boundaries and spread to other organs of the body. They are also named as neoplasm and malignant tumour [1]. Cancer is the second leading cause of death globally, with an estimated 1.8 million new cancer cases diagnosed and there were 606,520 cancer deaths worldwide in 2020[2]. Epigenetic regulations are one of the important factors in tumour initiation and progression. Among these, acetylation is the most important modification. The acetylation is controlled by two families of enzymes: histone acetyltransferases (HATs) and histone deacetylases (HDACs). Both of the enzymes exert their action on the amino group of lysine residues[3]. Epigenome is for the regulation of genetic information, which consists of covalent modifications of DNA and histone proteins. They are controlled by different enzymes known as writers, readers, and erasers and these enzymes sets a specific mark on chromatin. Any modifications are introduced by the writer proteins and then readers' enzymes recognize them and remodel them into chromatin structure which regulates the gene expression[4].

HDACs are known as eraser enzymes and are responsible for the deacetylation of acetyl groups from the lysine residues which leads to chromatin condensation, and transcriptional repression which further activates the tumorigenesis. So, HDAC inhibition results in a more open chromatin structure that promotes gene transcription which finally leads to growth arrest, differentiation, and apoptosis[5]. HDACs deacetylase both the histone and nonhistone proteins such as p53 and GATA-1 [6]. In human genome, 18 HDAC enzymes are identified and divided into four classes based on their homology to yeast HDACs: class I, II and IV are Zn^{2+} dependent, class III is NAD^{+} dependent. Class, I HDACs are related to yeast Rpd3 deacetylase or rpd3-like proteins and consist of HDAC1,2,3, and 8, localized in the nucleus. Class II HDAC family are homologous to histone deacetylase 1(Hda1) and divide into two subclasses, class IIA (HDAC4,5,7,9) and class IIB (HDAC6 and 10). They are localized in mitochondria and the nucleus. Class III HDACs also called sirtuins require an NAD^{+} for their enzymatic activity. Class IV family has only HDAC11 members and is localized in the nucleus[7].

A recent study showed that HDACs are overexpressed in various cancer types. Therefore, their inhibition provides an important and promising tool for developing novel anticancer drugs[8]. Till now, four HDACi (HDAC inhibitors) are approved-

Vorinostat (SAHA), Romidepsin (FK-228), Belinostat (PXD-101), Panobinostat (LBH-589) for the treatment of T-cell lymphoma, cutaneous T-cell lymphoma, multiple myeloma, specific types of blood cancer [5] and the structures are shown in Figure 1. According to their structural features, HDACi is classified into four classes: hydroxamates, cyclic peptides, short-chain fatty acids, and synthetic benzamides[9].

HDAC-2 acts as a transcriptional repressor that deacetylates lysine residues present at the N-terminal tail of histone proteins (H2A, H2B, H3, and H4). HDAC2 is the heterodimer of HDAC1, but it cannot bind to DNA, so they have to be transferred by the transcription factors such as YY1,SP1/SP3, and the tumour suppressor genes p53 and BRCA1. HDAC2 also be bound to DNA, with a part of the multiprotein corepressor complexes CoREST, mSin3, and NuRD[10]. HDAC-2 play a major role in various solid tumors including cutaneous t cell lymphoma, colorectal, prostate cancer, lung cancer, breast cancer, gastric cancer, liver cancer, and medulloblastoma, and is also expressed in hematological tumours[11]. Over the past few decades, the chromatin modification of HDAC has been a union of research for the treatment of cancer. Overactivity of HDAC will lead to cell proliferation, cell migration, and angiogenesis which is the characteristic form of cancer cells[12].

The main purpose of the study is to design, and develop the specific HDACi and evaluate its pharmacokinetic properties, dynamic studies, docking, and glide score of the different analogs which are further used as a novel HDACi for an HDAC-2 target.

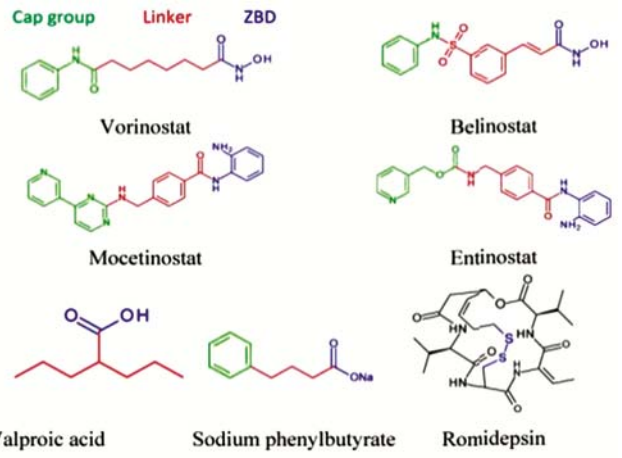

Figure 1 — FDA Approved drugs which acts as an inhibitor of HDAC-2

Experimental Section

Protein Preparation and grid generation

The structure of the human HDAC-2 Complex with inhibitor 4-(acetylamino) N- [2-amino 5-(thiophen-2-yl phenyl] benzamide (PDB ID: 4LY1) is retrieved from the Protein Data Bank (PDB) (https://www.rcsb.org/) was processed using the Protein Preparation Wizard of Schrodinger Wizard[13]. Resolution is 1.57 Å and residue number is 1107. It includes the addition of hydrogen bonds, assigning of bond orders, creating zero bond order to metals, creating disulfide bonds, filling in missing cap termini, missing loops, and missing side chains, which are modeled using Schrödinger Prime[14]. Water molecules beyond 5Å from het groups are deleted and het sates are generated using Epik at *p*H: 7$\pm$ 2. The protein is then reviewed and modified by selecting Chain A and het atom (20Y) within a 5Å radius of selected chains were retained for Docking Study and the water molecules and non-protein parts are removed. Then, states within 7+/- 2 are generated, after that it shows State Penalty in origin as0.0 kcal/mol and H-bond countas 3. The third step is to optimize the protein using PROPKA at *p*H 7. This was followed by energy minimization by applying a standard OPLS3e force field[15]. After minimization, the minimized protein is chosen for Grid Generation by using Glide Wizard of Schrödinger Software in which Dock ligand size is within 20 Å, finally, the Grid box develops within 20 Å and protein is ready for docking with ligands that are selected from different libraries for virtual screening.

Chemical library collection

We started with a few known HDACi with anticancer properties to establish the criteria for the selection of novel compounds. For this study, a different selection of libraries should be used. The structures of all reference compounds were retrieved from PubChem (http://pubchem.ncbi.nlm.nih.gov). To discover a new potent HDAC-2 inhibitor, we selected different chemical libraries such as ChEMBL (http://www.ebi.ac.uk/chembl/) database, and the NCI database (https://wiki.nci.nih.gov/display/NCIDTPdata/Chemical+Data) and Anticancer database.

Preparation of the small molecule library selection for virtual screening

From the chemical library, different derivatives were retrieved including CHEMBL database. From this, 3679 Assays were downloaded in 2D SDF format, and

HDAC-2 target compounds were downloaded. Other molecules were downloaded from the Anticancer and NCI/DTP databases, in which, 67382 compounds and ~2,46,542 compounds, resepctively are available. These structures were retrieved and prepared in two steps – by downloading the databases in smile format (2D format) and secondly, by the generation of 3D coordinates of compounds through CORINA (v 2.64) software package[16] by addition of missing hydrogen atoms and removal of small fragments. Approved HDAC-2 inhibitors are downloaded from PubChem. Ligands preparation was done by using Ligprep[17] wizard of Schrödinger Software. The ligand molecules were imported and neutralized by a neutralizer. Possible ionization states are generated at *p*H 7± 2 by using Epik Module[18]. The desalting and generation of tautomeric forms for each compound were used to ionize the molecules and a maximum of 32 confirmations are generated. After preparation, there were 4,34,850, 1,11,383, 4999 and 5691 structures in the NCI, Anticancer, ChEMBL assays, and HDAC-2 target analogs, and four reference compound libraries were also generated respectively for screening against 4LY1.

Molecular docking of chemical libraries against 4LY1

The ligand docking preparation was done by using Glide[19] Docking Wizard of Schrödinger Software 9.2. The previous grid was used for molecular docking of screened ligands. Molecular docking was performed consecutively in three steps- a)HTVS - for sorting Huge Chemical Libraries,b)SP (Standard Precision) - which uses less stringent functions, and c) XP (Extra Precision) - which gives a more rigorous penalty to the ligand poses for docking procedure using Maestro Schrodinger 9.2 [20]. In this, the number of poses per ligand should be 0.50 - 5 and per- residue interaction scores within 12 Å of grid atoms should be selected. The identified ligands with the best docking score, energy, glide score, and binding interaction against HDAC-2 Domain were further taken to analyze their binding effects through the MD study.

Screening of chemical library was performed through HTVS, then 10% of the obtained HTVS compounds SP mode were performed and after scoring, 10% of the SP compounds were performed in XP mode. The obtained best binding pose for each structure along with their docking score was saved for further post docking analysis.

Post docking analysis

The post docking analysis includes Ligplot after the selection of novel HDAC-2 inhibitors from a different library. The docking score of –9.0 kcal/mol was the highest docking score obtained from the reference compounds (Panobinostat). The analogs having docking score –9.0 kcal/mol or more were retained and others were discarded. From this top 10 molecules from CHEMBL, and 10 each from NCI and Anticancer library, ranked based on their respective docking score were reported. The different interactions of compounds with 4LY1 were further analyzed using Ligplot[21].

ADME properties and drug likeness

Qikprop[22] was utilized to perform and identify ADME properties along with drug-likeness. This helps to determine the efficiency and efficacy of the molecule. These properties are used to develop predictive ADME models and form the basis for property-based drug design.

Stability study through MD simulation

Based on the docking results and post docking analysis, the best-docked minimized complex structure was taken for the molecular dynamic simulation analysis using DESMOND[23]. For this purpose, we designed one compound which had the top docking score against 4LY1. A study was done in two steps- first by setting up the membrane by using TIP3P molecules, orthorhombic shape at 10 Å distance. The charge was neutralized by adding Na+ ions and 0.15 M NaCl was added as salt. Secondly, at NPT at 300 K temperature and 1 bar pressure, a 100 ns long MD simulation was carried out.

Results and Discussions

Molecular dockingofpotential HDAC-2 inhibitors from ChEMBL and different compound library

4LY1 has been downloaded and has three chains (Chain A, B, and C), Chain A was selected for docking studies. The docking score of CHEMBL assay compounds against HDAC-2 was found to vary between -14.078 to -9.216, Glide energy varies between -87.555 to -49.626, and the glides score from -14.078 to -9.223 as given in Table I. The structure and surface view of CHEMBL 4087539 and 3983272 are depicted in Figure 2 and Figure 3, respectively.

Similarly, the compounds from another library are also docked with 4LY1. It shows a docking score in

Table I — The top 10 scoring compounds after the virtual screening of ChEMBL assay compounds

S.no	Databases	Compound ID	Binding Affinity (Docking Score)	Glide Score (Kcal/mol)	Glide Energy(Kcal/mol)
1	ChEMBL	4087539	–14.078	–14.078	–87.555
2	ChEMBL	3983272	–13.004	–13.051	–71.336
3	ChEMBL	511432	–12.862	–12.955	–67.95
4	ChEMBL	3927842	–12.737	–12.74	–70.676
5	ChEMBL	3912393	–12.708	–12.758	–69.094
6	ChEMBL	1957458	–12.679	–12.68	–75.69
7	ChEMBL	2057820	–12.481	–12.482	–77.984
8	ChEMBL	2403475	–11.978	–12.168	–58.811
9	ChEMBL	3966973	–11.299	–11.411	–52.677
10	ChEMBL	568586	–10.308	–10.316	–52.779

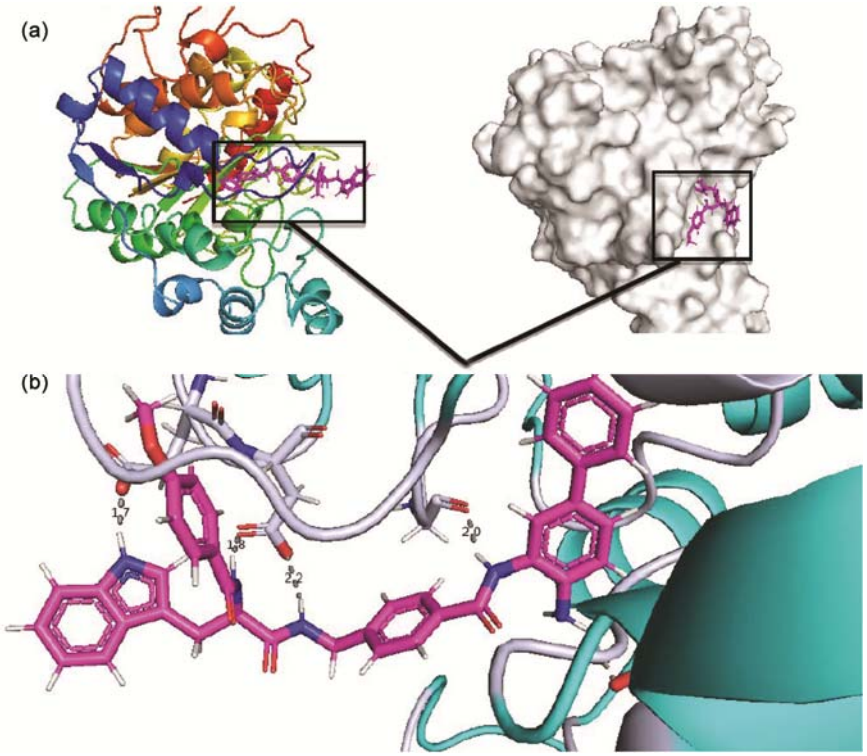

Figure 2 — The docked pose of top scoring compound, CHEMBL4087539 with HDAC-2 (PDB ID 4LY1), (a) Far view of HDAC-2 with inhibitor CHEMBL4087539 (Left) and surface view of HDAC-2 with inhibitor CHEMBL4087539 and (b) close view of HDAC-2 with inhibitor CHEMBL4087539

the range of -12.083 to -10.733 and predicted glide energy in the range of -72.591 to -57.18 and a glide score of -12.392 to -10.733 as given in Table II.

Ligplot analysis

Based on the inhibition experiments with HDAC-2, two residues Phe 155 and Cys 156 were found to play an important role in inhibition. The top docking score results show the residues list which was designed from Ligplot. By analysing top compounds with the Ligplot, it shows that Pro 34, His 33, Phe 155, Tyr 29, Phe 114, Met 35, Cys 156, Arg 39, Gly 143, Gly 305, Leu 144, Gly 306, Phe 210, Leu 276 and His 183 are forming a more hydrophobic interactions from chemical databases listed in Table III. These observations suggested that the identified compounds perform as better inhibitors of HDAC-2 than the reference compounds. The CHEMBL 4087539 shows hydrogen bonding interaction within the range of 2.67 - 3.15 Å as shown in Figure 4a and CHEMBL 3983272 forms hydrogen bond within the range of 2.76 - 3.06 Å as shown in Figure 4b. Molecular Representation of ChEMBL, NCI, Anticancer Library are given in Table IV.

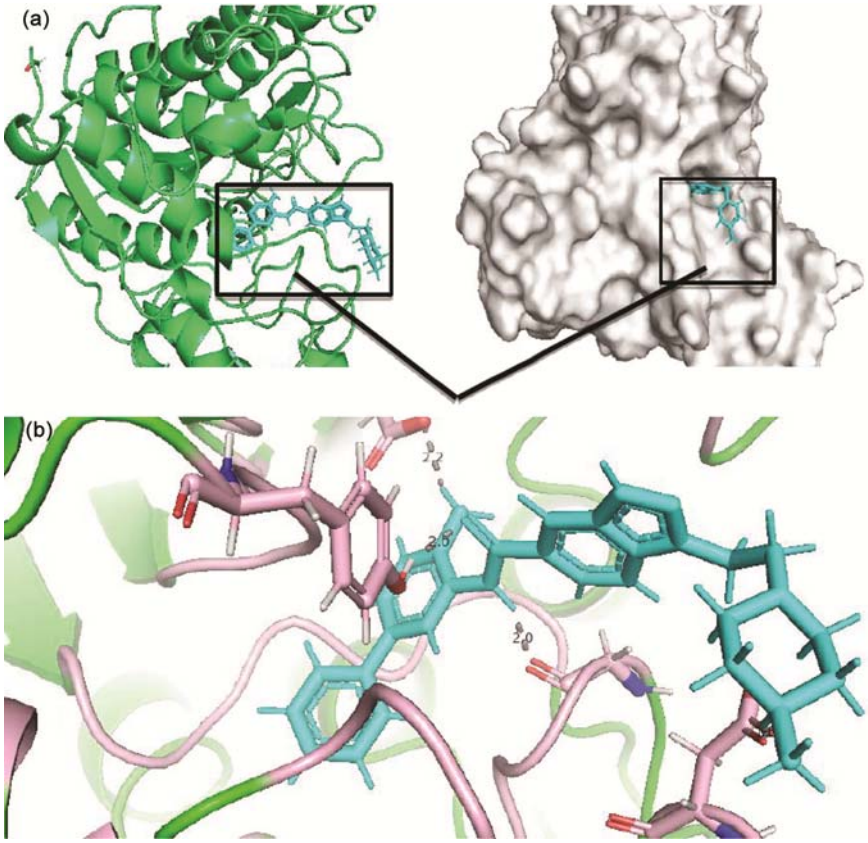

Figure 3 — The docked pose of second top scoring compound CHEMBL3983272, with HDAC-2 (PDB ID 4LY1), (a) Far view of Structure of HDAC-2 with inhibitor CHEMBL3983272 (Left) and surface view of HDAC-2 with inhibitor CHEMBL3983272 and (b) close view of structure of HDAC-2 with inhibitor CHEMBL3983272.

Table II — The top 10 scoring compounds after the virtual screening of NCI and anticancer chemical libraries

S.no	Databases	Compound ID	Binding Affinity (Docking Score)	Glide score (Kcal/mol)	Glide Energy
1	NCI	106858	–12.083	–12.392	–72.591
2	NCI	334320	–11.555	–11.854	–55.653
3	NCI	96948	–11.547	–11.634	–56.788
4	NCI	704415	–11.524	–11.524	–58.399
5	NCI	337734	–11.487	–11.668	–54.268
6	Anticancer	42046	–11.126	–11.126	–53.465
7	Anticancer	37879	–11.039	–11.039	–56.28
8	Anticancer	25884	–10.832	–10.832	–56.951
9	Anticancer	22646	–10.749	–10.749	–57.987
10	Anticancer	66654	–10.733	–10.733	–57.18

Protein-ligand interactions

The interaction of HDAC-2 with its analogs and the binding poses of all interactions are shown in Figure 1S.

MD Simulation

MD simulations are done to evaluate how ligands are interacting with the receptor and whether they are showing stable interactions or not. The binding stability was identified from the top docked scored compound from ChEMBL (CHEMBL4087539) and was evaluated in terms of free energy of binding against the (4LY1) active site. All the analysis are shown in Figure 5 from MD simulation of HDAC-2 protein (4LY1) with CHEMBL4087539 at 100ns

There is no difference in the RMSD between native protein and with inhibitor, showing that complex is stable with the inhibitors also. The radius of gyration of the native protein is 1.9 nm but gyration of the protein with inhibitors is 1.75 nm, this shows that

Table III — List of residues that are involved in interaction with the ligand both hydrogen bonding and non-bonded

S. No.	Databases	Compound ID	H-bond interactions	Hydrogen bond range (Å)	Hydrophobic interactions; no. of interactions
1	ChEMBL	4087539	Glu103, Asp104, Tyr308, Asp179, His146, Asp186, Asp181, His145, Gly154	2.67-3.15	Gly 32, Pro 34, His 33, Phe 155, Tyr 29, Arg 39, Phe 114, Gly 306, Gly305, Met 35, Cys 156, Gly 143, Leu 144, His 183, Phe 210, Leu 276; 16
2	ChEMBL	3983272	Glu103, Gly154, Asp181, His146, His145, Asp186, Asp179,Tyr308, Asp 104	2.76-3.06	Pro 34, His 33, Phe 155, Tyr 29, Phe 114, Met 35, Cys 156, Arg 39, Gly 143, Gly 305, Leu 144, Gly 306, Phe 210, Leu 276, His 183;15
3	ChEMBL	511432	Phe210,Ala141, Gly142,Tyr308,Gly154, His183	2.81-3.30	Asp104,Phe155,Tyr308,His146,Cys 156,Gly306,Met35,Leu144,Tyr29, Arg39,Phe114,Gly304,Ile40,Asp18 1,Gly143,His145; 16
4	ChEMBL	3927842	Gly154,his145,his146,tyr3 08,his183	1.08-2.94	Asp104,phe210,phe155,gly306,asp 181,gly143,cys156,gly305,gly142,a rg39,ala141,phe114,tyr29,leu144,m et35,leu276; 16
5	ChEMBL	3912393	Asp181,his145,his146,gly 154,tyr308,his183,ohe210	1.99-2.70	Ala141,phe114,leu144,tyr29,met35, cys156,leu276,phe155, ,gly306,gly143,gly305,arg39,ile40; 13
6	ChEMBL	1957458	Phe210,Ala141, Gly142,Tyr308,Gly154, His183	1.98-2.98	Asp104,Phe155,Tyr308,His146,Cys 156,Gly306,Met35,Leu144,Tyr29, Arg39,Phe114,Gly304,Asp181,Gly 143,His145;15
7	ChEMBL	2057820	Asp181,his145,his146,gly 154,his183,tyr29	2.00-2.92	Met35,leu144,phe114,ala141,arg39, gly142,gly305,cys156,gly143,gly30 6,gln265,pro34,his33,glu103,asp10 4,phe210,phe155,leu276;18
8	ChEMBL	2403475	Asp104,His145, Gly 154	2.76-3.09	Leu 276, Phe 155, His 183, Tyr 29, Cys 156, Met 35, Leu 144, Arg 39, Gly 305. Gly 306, Tyr 308, His 146, Phe 210; 14
9	ChEMBL	3966973	Asp 104, Asp 269, Tyr 308, Asp 181	1.57-3.01	Glu 103, Pro 34, Gly 143, Met 35, His 146, Gly 306, Cys 156, His 145, Gly 154, Phe 155, Gly 305, Leu 276, His 183, Pro 310,leu144; 15
10	ChEMBL	568586	Asp 104, Asp 269, Tyr 308, Asp 181,gly154	1.76-2.69	Glu 103, Pro 34, Gly 143, Met 35, His 146, Gly 306, Cys 156, His 145, Gly 154, Phe 155, Gly 305, Leu 276, His 153, Pro 210; 14
11	NCI	106858	Tyr 308, Gly 154, Asp 104	2.62-2.93	Gly305,gly306,his183,his146,leu14 4,arg39,phe114,gly142,gly143,met 35,pro34,his33,gly32,phe155,cys15 6,phe210,tyr29,phe210,phe155;19
12	NCI	334320	Gly154,asp104	1.85-2.52	Phe210,asp104,leu276,arg39,phe11 4,tyr29,gly142,gly143,leu144,his14 5,his146,gly306,gly305,phe155,cys 156,gly154;16
13	NCI	96948	Gly154,tyr308,his145	2.19-3.03	Phe210,phe155,leu276,his145,asp1 81,cys156,met35,gly305,gly142,leu 144,arg39,phe114,tyr29,asp104;14

(*Contd.*)

Table III — List of residues that are involved in interaction with the ligand both hydrogen bonding and non-bonded (*Contd.*)

S. No.	Databases	Compound ID	H-bond interactions	Hydrogen bond range (Å)	Hydrophobic interactions; no. of interactions
14	NCI	704415	Gly154,his145	1.31-2.75	Tyr29,phe114,ala141,leu144,arg39,gly142,met35,cys156,gly305,asp269,asp181,gly306,his183,tyr308,phe155,phe210,leu276;17
15	NCI	337734	His145	1.67-2.60	His183,gly154,his146,tyr308,asp269,gln265,asp181,gly306,gly143,leu144,gly305,cys156,gly142,arg39,met35,ala141,phe114,phe155,phe210,asp104;16
16	Anticancer	42046	Gly154, Tyr308	2.73-3.11	Phe 210, Phe 155, Leu 276, Cys 156, Tyr 29, Met 35, Arg 39, Leu 144, Gly 143, His 145, Gly 305, Gly 306, His 146, His 183;14
17	Anticancer	37879	Gly154	3.00	Tyr 209, phe 210, leu 276, phe 155, cys 156, tyr 29, met 35, phe 114, arg 39, leu 144, gly 143, his 146, gly 305, gly 306, his 183,tyr 308;16
18	Anticancer	25884	Tyr308, gly154	1.93-2.83	leu276,gly306,gly305,met35,tyr29,phe114,tyr209,phe210,cys156,phe155,his146,leu144,gly143,gly142,ala141;15
19	Anticancer	22646	Tyr308, gly154	1.87-1.93	Phe114,tyr29,met35,leu276,tyr308,arg39,tyr209,phe210,cys156,phe155,his146,leu144,gly143,ala142;14
20	Anticancer	66654	Tyr308, gly154	1.93	met35,his183,tyr308,tyr29,gly306,gly305,ile40,phe114,arg39,ala141,gly143,leu144,his146,cys156,phe155,phe210;16

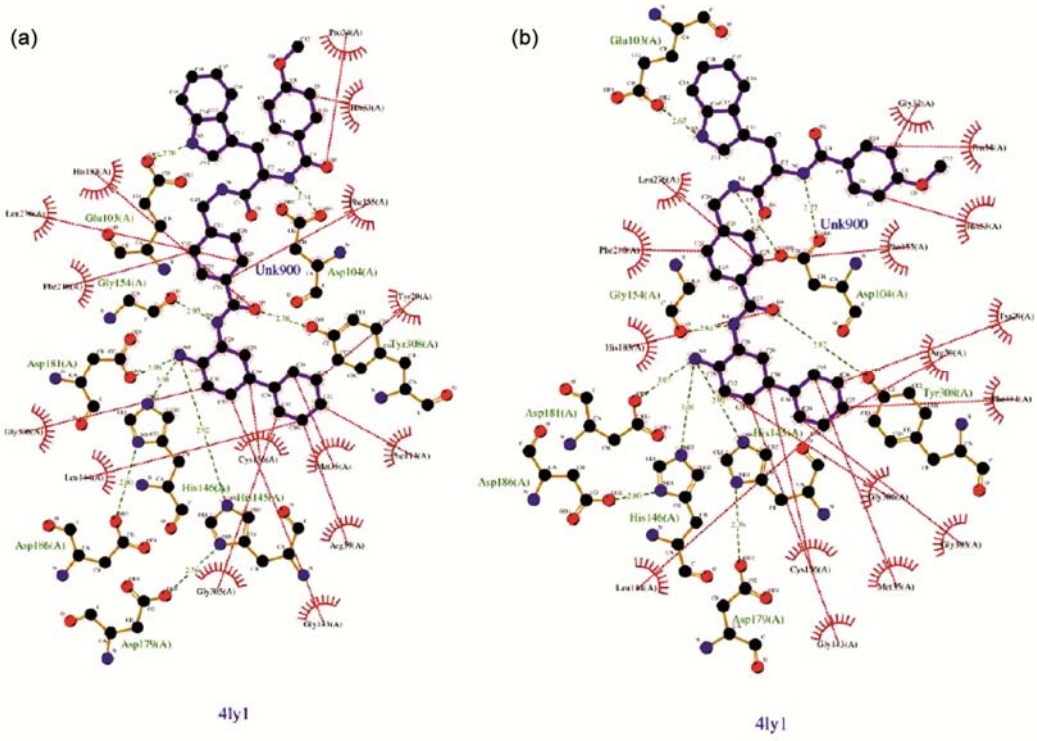

Figure 4 — Two dimensional ligand interaction diagram, (a) interaction with CHEMBL 4087539 and (b) interaction with CHEMBL 3983272

Table IV — IUPAC name and structure of ChEMBL, NCI, anticancer compounds. The IUPAC name, structure was retrieved from the Chem Draw

S.no	Databases	Compound Id	Structure	IUPAC
1	ChEMBL	4087539	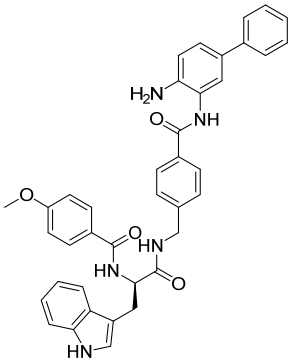	(R)-4-((3-(1*H*-indol-3-yl)-2-(4-methoxybenzamido)propanamido)methyl)-N-(4-amino-[1,1'-biphenyl]-3-yl)benzamide
2	ChEMBL	3983272	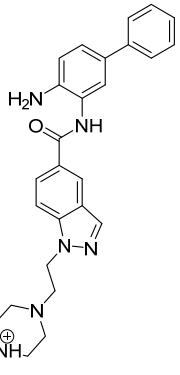	4-(2-(5-((4-amino-[1,1'-biphenyl]-3-yl)carbamoyl)-1*H*-indazol-1-yl)ethyl)-1-methylpiperazin-1-ium
3	ChEMBL	511432	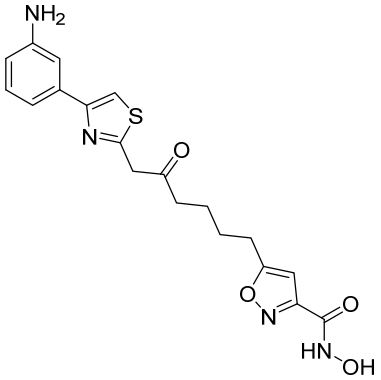	5-(6-(4-(3-aminophenyl)thiazol-2-yl)-5-oxohexyl)-N-hydroxyisoxazole-3-carboxamide
4	ChEMBL	3927842	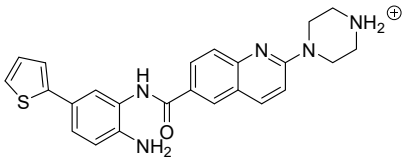	4-(6-((2-amino-5-(thiophen-2-yl)phenyl)carbamoyl)quinolin-2-yl)piperazin-1-ium
5	ChEMBL	3912393	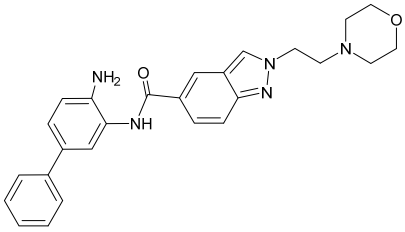	N-(4-amino-[1,1'-biphenyl]-3-yl)-2-(2-morpholinoethyl)-2*H*-indazole-5-carboxamide

(*Contd.*)

Table IV — IUPAC name and structure of ChEMBL, NCI, anticancer compounds. The IUPAC name, structure was retrieved from the Chem Draw (*Contd*.)

S.no	Databases	Compound Id	Structure	IUPAC
6	ChEMBL	1957458	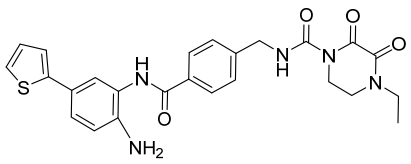	N-(4-((2-amino-5-(thiophen-2-yl)phenyl)carbamoyl)benzyl)-4-ethyl-2,3-dioxopiperazine-1-carboxamide
7	ChEMBL	2057820	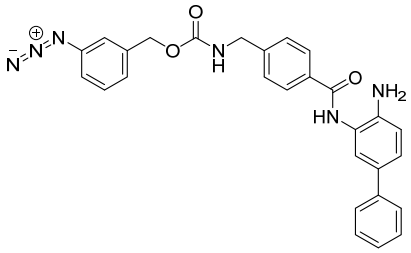	3-azidobenzyl (4-((4-amino-[1,1'-biphenyl]-3-yl)carbamoyl)benzyl)carbamate
8	ChEMBL	2403475	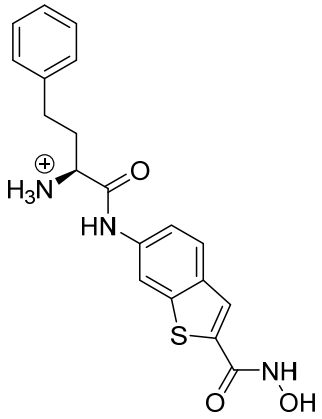	S)-2-((2-(hydroxycarbamoyl)benzo[b]thiophen-6-yl)amino)-5-phenylpent-1-en-3-aminium
9	ChEMBL	3966973	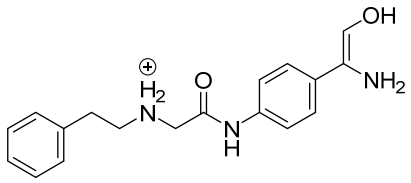	(Z)-2-((4-(1-amino-2-hydroxyvinyl)phenyl)amino)-2-oxo-N-phenethylethan-1-aminium
10	ChEMBL	568586	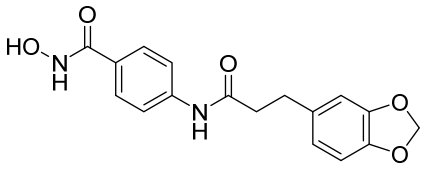	4-(3-(benzo[d][1,3]dioxol-5-yl)propanamido)-N-hydroxybenzamide
11	NCI	106858	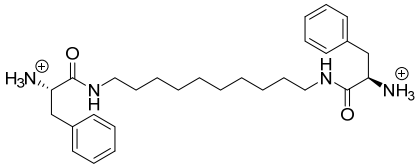	(S)-1-((10-((R)-2-ammonio-3-phenylpropanamido)decyl)amino)-1-oxo-3-phenylpropan-2-aminium

(*Contd*.)

Table IV — IUPAC name and structure of ChEMBL, NCI, anticancer compounds. The IUPAC name, structure was retrieved from the Chem Draw (*Contd*.)

S.no	Databases	Compound Id	Structure	IUPAC
12	NCI	334320	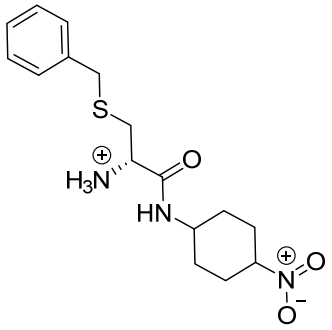	(S)-3-(benzylthio)-1-((4-nitrocyclohexyl)amino)-1-oxopropan-2-aminium
13	NCI	96948	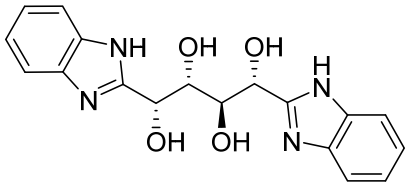	(1R,2R,3S,4R)-1,4-bis(1*H*-benzo[d]imidazol-2-yl)butane-1,2,3,4-tetraol
14	NCI	704415	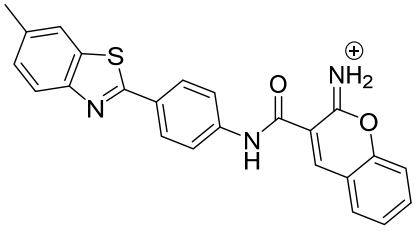	3-((4-(6-methylbenzo[d]thiazol-2-yl)phenyl)carbamoyl)-2*H*-chromen-2-iminium
15	NCI	3377342	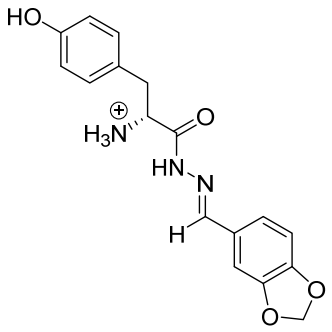	(R,E)-1-(2-(benzo[d][1,3]dioxol-5-ylmethylene)hydrazinyl)-3-(4-hydroxyphenyl)-1-oxopropan-2-aminium
16	Anticancer	42046	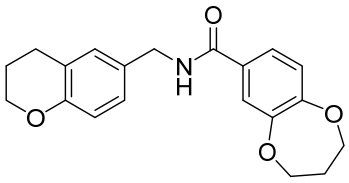	N-(chroman-6-ylmethyl)-3,4-dihydro-2*H*-benzo[b][1,4]dioxepine-7-carboxamide
17	Anticancer	37879	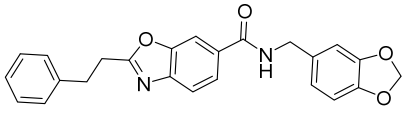	N-(benzo[d][1,3]dioxol-5-ylmethyl)-2-phenethylbenzo[d]oxazole-6-carboxamide

(*Contd*.)

Table IV — IUPAC name and structure of ChEMBL, NCI, anticancer compounds. The IUPAC name, structure was retrieved from the Chem Draw (*Contd*.)

S.no	Databases	Compound Id	Structure	IUPAC
18	Anticancer	25884	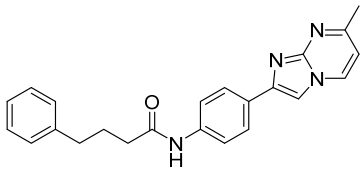	N-(4-(7-methylimidazo[1,2-a]pyrimidin-2-yl)phenyl)-4-phenylbutanamide
19	Anticancer	22646	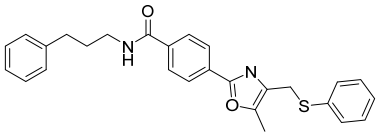	4-{5-methyl-4-[(phenylthiol)methyl]-1,3-oxazol-2-yl}-N-(3-phenylpropyl) benzamide
20	Anticancer	66654	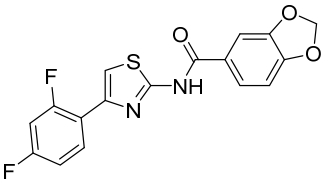	N-(4-(2,4-difluorophenyl)thiazol-2-yl)benzo[d][1,3]dioxole-5-carboxamide

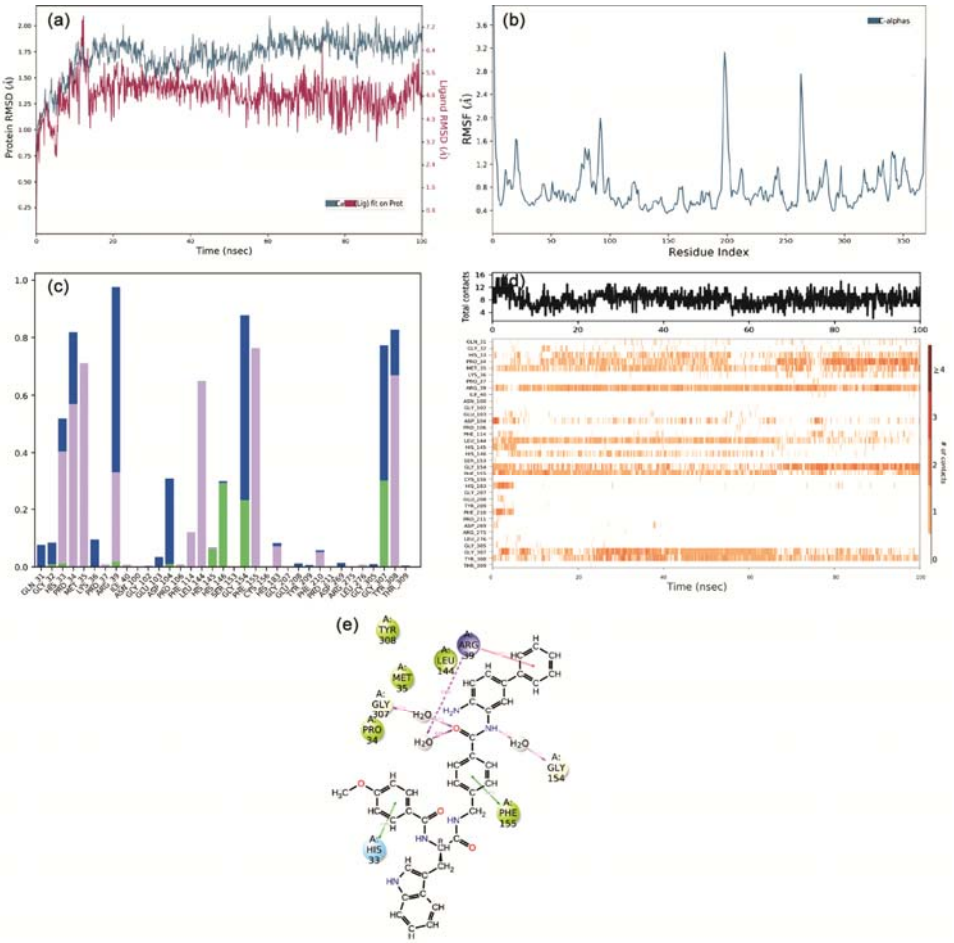

Figure 5 — (a) RMSD of protein ligand complex. The simulations were run for 100 ns with OPLS 2005 forcefield. The figure shows the convergence of molecular trajectories and the protein ligand complex is in metadynamic stable state, (b) RMSF of protein residues for the simulation of 100 ns, (c) Protein- Ligand Interactions diagram showing the H-bond, ionic, hydrophobic and water bridge interaction with histone deacetylase, (d) Heat map showing the number of contacts with histone deacetylase and (e) 2 dimensional interaction diagram during molecular dynamics. Interaction that occur more than 30.0% of the simulation time in the selected trajectory (0.00 through 100.00 ns) are shown

protein is more compact when it is bound with an inhibitor as compared to the native form. The blue color represents protein (4LY1), Pink color represents Ligand.

RMSF of the native protein is ranging between 0.7 nm to 3.6 nm and RMSF of protein with inhibitors is ranging between 0.9 nm to 2.9 nm. This shows that there are more fluctuations in the backbone when it is in the native form, but with inhibitors, it is showing fewer fluctuations. The solvent-accessible surface area of the native protein is 140 nm^2, and 125 nm^2 with inhibitors.

The top panel shows the total number of specific contacts the protein makes with the ligand throughout the trajectory. The bottom panel shows which residues interact with the ligand in each trajectory frame. Some residues make more than one specific contact with the ligand, which is represented by a darker shade of orange, according to the scale to the right of the plot.

Green color represents H- Bonding which shows the distance of 2.5 Å between the donor and acceptor atoms, a donor angle of ≥120° between the donor-hydrogen-acceptor atoms; and an acceptor angle of ≥90° between hydrogen-acceptor-bonded atoms. Purple color indicates hydrophobic Interactions which demonstrates π - cation — aromatic and charged groups within 4.5 Å; π-π — two aromatic groups stacked face-to-face or face-to-edge; other — a non-specific hydrophobic side chain within 3.6 Å of a ligand's aromatic or aliphatic carbons.

The blue color represents water bridges which indicates protein-water or water-ligand H-bond with a distance of 2.8 Å between the donor and acceptor atoms and a donor angle of ≥110° between the donor-hydrogen-acceptor atoms and an acceptor angle of ≥90° between the hydrogen-acceptor-bonded atoms .

ADMET Property

ADMET property of reference compounds of HDACi and top 20 analogs from a different library related to the reference compound is used as standard listed in Table V and Table VI. Lipinski rule is applied for the physicochemical properties: molecular weight ≤ 500 Daltons, hydrogen bond donor ≤ 5, hydrogen bond acceptor ≤ 10, and an octanol-water partition coefficient log P ≤ 5.

GOLD Scoring

The analogs are also screened with another process through Gold software. From this, each of the different libraries was earlier used and screened against the 4LY1. After docking, the top 10 compounds were screened and gold fitness scores from these libraries are listed in Table VII. The reference compound has a gold fitness score from 54.7584 to 85.7445 kcal/mol. Hence the compounds

Table V — Representation of physicochemical properties for reference drugs

S. No	Compound	Log P	Mol. wt	H bond donor	H bond acceptor
1	Panobinostat	3	349.4	4	3
2	Vorinostat	1.9	264.32	3	3
3	Entinostat	2	376.4	3	5
4	Belinostat	1.7	318.3	3	5
5	Romidepsin	2.2	540.7	4	8

Table VI — ADMET prediction of 20 optimized compounds

Databases	Compound Id	mol_Wt.	donorHB	acceptHB	QPlogP o/w	QPlogS	QPlog HERG
ChEMBL	4087539	312.324	2	7.95	1.424	–3.614	–5.961
ChEMBL	3983272	454.574	2.5	8.5	3.551	–4.571	–9.0223
ChEMBL	511432	401.439	4.5	10	0.558	–4.512	–6.504
ChEMBL	3927842	429.539	3.5	6.5	3.769	–5.748	–7.839
ChEMBL	3912393	441.532	2.5	8.7	3.417	–4.662	–7.802
ChEMBL	1957458	491.564	2.5	9	3.242	–7.109	–6.098
ChEMBL	2057820	492.536	3.5	8.5	4.228	–8.515	–9.079
ChEMBL	2403475	369.437	5	7.7	1.21	–3.069	–7.198
ChEMBL	3966973	312.371	5	7.2	0.985	–2.244	–7.29
ChEMBL	568586	328.324	3	8.2	1.118	–3.138	–5.458
NCI	106858	466.665	6	7	2.976	–3.025	–6.361
NCI	334320	331.389	3	5	2.216	–3.302	–7.074
NCI	96948	354.365	6	9.8	0.588	–2.999	–6.477
NCI	704415	411.477	1	4.5	5.281	–7.458	–7.474
NCI	337734	327.339	4	5.75	1.483	–2.007	–6.224
Anticancer	42046	339.39	1	4.75	4.012	–5.228	–5.352
Anticancer	37879	400.433	1	6	4.582	–5.773	–6.887
Anticancer	25884	370.453	1	5	5.101	–7.004	–7.461
Anticancer	22646	442.575	1	5	6.879	–8.643	–8.321
Anticancer	66654	360.334	1	5.5	3.569	–4.88	–5.616

Table VII — Docking of HDAC-2 with databases and their binding affinities through GOLD

S.No	Compound ID	Gold Fitness Score
1	Compound 1 (ChEMBL 4087539)	115.3324
2	Compound 2 (ChEMBL3983272)	111.6985
3	Compound 3 (ChEMBL511432)	111.2894
4	Compound 4 (ChEMBL 2403475)	99.2299
5	Compound 5 (ChEMBL3927842)	94.2941
6	Compound 6 (ChEMBL3966973)	92.2648
7	Compound 7 (NCI 106858)	92.1422
8	Compound 8 (Anticancer 37879)	89.6549
9	Compound 9 (NCI 334320)	89.2641
10	Compound 10 (ChEMBL 2023526)	87.9785

which have a high gold score with the reference compounds are listed, while others were discarded. It shows that the gold fitness score of 10 analogs is 115.3324 kcal/mol to 87.9785 kcal/mol.

Conclusions

The HDAC-2 domain (residue range 1-369) was modelled using the comparative modelling approach. The molecules were successfully docked to protein (4LY1) to get an idea about their possible interaction with the structures obtained from the different chemical libraries. The current study demonstrates that the different potential inhibitors of HDAC-2 (from ChEMBL, NCI, and anticancer databases) were identified through virtual screening through Schrodinger. Out of which 10 best-docked analogs were selected from ChEMBL and 10 from NCI and anticancer databases and compared with the reference drug. Further, post docking analysis of 20 compounds with the Ligplot shows that residues are forming a hydrophobic interactions, hydrogen bond interactions, and hydrogen bonds. Finally, the ADMET property of these analogs which follows the Lipinski rule was determined. Then, another screening of compounds using Gold software was performed in which the top 10 best-docked compounds were listed. The study aims to understand drug-receptor interaction and pharmacokinetic parameters of HDAC-2 analogs. The highest docked compound was observed in the stability study through MD simulation with the protein showing that the complex is stable with the selected inhibitor. From this, the study concludes that some of the modified analogs were better than commercial drugs. In future research work, analogs can be used further in clinical trials to test their effectiveness and for social benefits thus reducing the time and cost of drug discovery.

Supplementary Information

Supplementary information is available in the website http://nopr.niscpr.res.in/handle/123456789/58776.

Conflict of interest

There is no conflict of interest to declare.

References

1 https://www.who.int/health-topics/cancer.
2 https://www.cancer.org/research/cancer-facts-statistics/all-cancer-facts-figures/cancer-facts-figures-2020.html
3 Yang F, Zhao N, Ge D & Chen Y, *RSC Adv*, 9 (2019) 19571.
4 Bora G, Sarı S, Taşkor G, Dalkara S & Erdem-Yurter H, *J Res Pharm*, 23 (2019) 952.
5 Wang Y, Su L, Wang Q, Zhang L & Luan Y, *Drug Dev Res,* 81 (2019) 52.
6 Alsawalha M, Bolla S R, Kandakatla N, Srinivasadesikan V, Veeraraghavan V P & Surapaneni K M, *Bioinformation*, 15 (2019) 380.
7 Mottamal M, Zheng S, Huang T L, & Wang G, *Molecules,* 20 (2015) 3898.
8 Asfaha Y, Schrenk C, Avelar L A A, Lange F, Wang C, Bandolik J J, Hamacher A, Kassack M U & Kurz T, *Bioorg Med Chem*, 28 (2020) Article 115108.
9 Lakshmaiah K C, Jacob L A, Aparna S, Lokanatha D & Saldanha S C, *J Cancer Res Ther*,10 (2014) 469.
10 http://atlasgeneticsoncology.org/gene/40803/hdac2-(histone-deacetylase-2)Rikiishi H, *Cancers*, 2 (2010) 2026.
11 Choubey S K & Jeyakanthan J, *J Mol Graph Model*, 70 (2016) 54.
12 Protein Preparation Wizard, Epik, Schrödinger, LLC, NY, 2016.
13 Prime, Schrödinger, LLC, NY, 2016.
14 Jorgensen W L, Maxwell D S & Tirado-rives J, *J Am Chem Soc*, 118 (1996) 11225.
15 Sadowski J, Schwab C H & Gasteiger J, *CORINA 3D Structure Generator*, Version 3.0, Molecular Networks GmbH Computerchemie, March 2003.
16 LigPrep, Schrödinger, LLC, New York, NY, 2020.
17 Epik, Schrödinger, LLC, New York, NY, 2020.
18 Glide, Schrödinger, LLC, New York, NY, 2020.
19 Maestro, Schrödinger, LLC, New York, NY, 2020.
20 https://www.ebi.ac.uk/thornton-srv/software/LIGPLOT/
21 QikProp, Schrödinger, LLC, New York, NY, 2020.
22 Desmond Molecular Dynamics System, D. E. Shaw Research, New York, NY, 2020. Maestro-Desmond Interoperability Tools, Schrödinger, New York, NY, 2020.